AN ANALYTICAL MODEL FOR PREDICTION OF THE STEADY STATE CREEP DEFORMATIONS AND STRESSES OF SHORT FIBER COMPOSITES

M. Mondali, A. Abedian, A. Ghavami
Department of aerospace engineering, Sharif University of Technology, P.O. Box 11365-8639, Azadi Avenue, Tehran, Iran

Keywords: *Short fiber composites, Shear lag theory, creep, Analytical modeling, FEM*

Abstract

A new analytical model based on the shear-lag theory is developed for stress analysis and steady state creep deformation of short fiber composites subjected to an applied axial load. A perfect fiber/matrix interface is assumed and an exponential law is considered for describing the steady state creep behavior of the matrix material. The matrix stress field components obtained from the proposed analytical solution satisfies the equilibrium and constitutive creep equations. Also, the obtained axial stress in the fiber in an average form satisfies the equilibrium requirements within the fiber and between the fiber and the matrix. Moreover, the above stress field components satisfy well the overall boundary conditions including the surface conditions, the interface continuity conditions, and the axial force equilibrium conditions. These analytical results are then validated by the FEM modeling. Interestingly, good agreements are found between the analytical and numerical predictions for all the stress, strain rate, and displacement rate components.

2 Introduction

The increasing application of short fiber composites at high stress and high temperature requires a through knowledge of their creep characteristics and deformation mechanisms. In recent years, extensive investigations have been conducted to determine the creep properties of short fiber composites [1-7], which is of great importance in practical engineering. The wide range of available composite materials for a specific purpose makes it difficult to evaluate experimentally the creep properties of these materials. Thus the use of analytical or numerical methods is unavoidable. Although, the numerical methods are quick and easy, the analytical approaches provide enough confidence on the predicted results.

Over the past few decades, different analytical models have been developed for prediction of the second stage creep rate and also stress states in short fiber composites. In most of the studies, the stress transfer between the matrix and the fiber is considered to be the most important mechanism governing the creep behavior of these materials. Majority of the analytical models are one-dimensional and are typically based on the shear-lag theory [1-6]. In these models, the concepts employed by Cox [8] have been used assuming elastic short fibers and exponential or power law creep matrix.

What for sure is missing, is an analytical solution of creep behavior of short fiber composites based on the well know shear-lag theory, which can satisfy all the constitutive and equilibrium equations and match the existing FEM results. Also, a little progress has been made in development of a tool for analysis of stress states in aligned short fiber composites.

In general, the short-comings of the available analytical models could be highlighted as follows:

- Most of these models are available for just one type of creep law and some of them provide unsatisfactory results by changing the law.

- The results obtained by the analytical 1-D shear-lag based models don't satisfactorily correlate the FEM results.
- Calculation of the creep strain rate has been the main goal of most of these models and due to using shear-lag theory only $\overline{\sigma}_z^f$, $\overline{\sigma}_z^m$ and τ_i as a function of z could be obtained. Note that $\overline{\sigma}_z^f$, $\overline{\sigma}_z^m$ are the respective average axial stress in the fiber and matrix and τ_i is the interfacial shear stress. In fact, these models are unable to calculate other stress components and also the displacement rates of the composite. Moreover, by these models, the variation of stress and displacement rate fields with r and z is not in hand.
- Generally, this problem involves with two equilibrium equations and a constitutive law, which consists of four equations [9]. In 1-D shear-lag based models only one of the equilibrium equations is used. Also, instead of the constitutive equations, the simple velocity relations of the flowing matrix are used for calculating the strain rate of the composite in steady state creep stage.

Normally, with the axisymmetric assumption of the problem, satisfaction of all the equilibrium and constitutive equations even for the elastic state of the composite constituents are hardly occurred. The exceptions come here with only considering several approximating and reducing assumptions [10-14]. It should be noted that in elastic case the elastic modulus of the matrix (E) appears in the constitutive equations, which is a constant. However, when the matrix ends up in the steady state creep stage, as will be discussed later, instead of E_m the complicated term of $\dot{\varepsilon}_e / 2\sigma_e$ appears in the matrix constitutive equations. Note that here σ_e and $\dot{\varepsilon}_e$, which are the equivalent stress and equivalent strain rate of the matrix respectively will be functions of r and z coordinates.

In the present work, an analytical solution for prediction of the steady state creep behavior of short fiber composites based on shear-lag theory is offered. Here, an axisymmetric unit cell representing a fiber with its surrounding matrix as two coaxial cylinders is assumed. The proposed solution technique satisfies all the equilibrium and the constitutive equations along with all the existing boundary conditions. This model is capable for providing the stress state inside the composite, i.e. radial, circumferential, axial and shear stress components, as well as the radial and axial displacement rates as functions of r and z coordinates. For verification of the solution method, the SiC/6061Al composite is selected as a case study and the results will be compared with the FEM and other analytical available results in [4,7].

3 Model development

2.1 Composite model

The cylindrical unit cell depicted in Fig.1 has been used by many researchers [4,7,10-14] to model a short fiber composite.

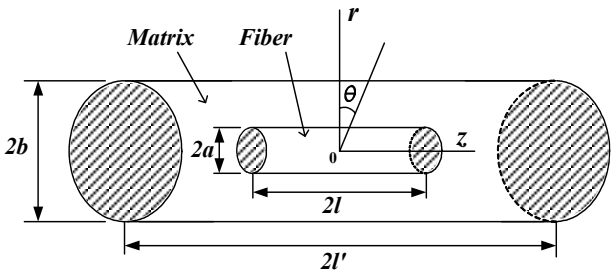

Fig. 1. Schematic presentation of the unit cell

In this model it is assumed that a cylindrical fiber with a radius a and a length $2l$ is embedded in a coaxial cylindrical matrix with an outer radius b and a length $2l'$. The volume fraction and aspect ratio of the fiber are defined as f and $s = l/a$, respectively. Also, in this study, $k = \dfrac{l'/b}{l/a}$ is considered as a parameter related to the geometry of the unit cell. An applied axial stress σ_0 is uniformly imposed on the end faces of the unit cell (at $z = \pm l'$). The cylindrical polar coordinate system (r, θ, z) is used with the origin located at the center of the unit cell. Due to symmetry in geometry, loading, and boundary conditions, the analysis is performed only on half of the unit cell (i.e. $0 \le z \le l'$).

For the purpose of analysis, the following further assumptions are made:

i) Steady state condition of stress is assumed.
ii) Elastic deformations are small and are neglected as compared to creep deformations.
iii) The fibers behave elastically during the analysis and the steady state creep behavior of the matrix is described by an exponential law as given in Eq. (1),

$$\dot{\varepsilon}_e = A\exp(\sigma_e / B) \qquad (1)$$

iv) A perfect fiber/matrix interface is considered.

2.2 Governing equations and relations

The governing equations for the axisymmetric problem considering the cylindrical coordinates (r,θ,z) are obtained as

$$\frac{\partial\sigma_z}{\partial z}+\frac{\partial\tau_{rz}}{\partial r}+\frac{\tau_{rz}}{r}=0 \qquad (2a)$$

$$\frac{\partial\sigma_r}{\partial r}+\frac{\partial\tau_{rz}}{\partial z}+\frac{\sigma_r-\sigma_\theta}{r}=0 \qquad (2b)$$

The generalized constitutive equations for creep deformation of the matrix material in r,θ and z directions [9] are

$$\dot{\varepsilon}_r=\frac{\partial\dot{u}}{\partial r}=\frac{\dot{\varepsilon}_e}{2\sigma_e}[2\sigma_r-\sigma_\theta-\sigma_z] \qquad (3a)$$

$$\dot{\varepsilon}_\theta=\frac{\dot{u}}{r}=\frac{\dot{\varepsilon}_e}{2\sigma_e}[2\sigma_\theta-\sigma_r-\sigma_z] \qquad (3b)$$

$$\dot{\varepsilon}_z=\frac{\partial\dot{w}}{\partial z}=\frac{\dot{\varepsilon}_e}{2\sigma_e}[2\sigma_z-\sigma_r-\sigma_\theta] \qquad (3c)$$

$$\dot{\varepsilon}_{rz}=\frac{1}{2}\left(\frac{\partial\dot{u}}{\partial z}+\frac{\partial\dot{w}}{\partial r}\right)=\frac{3\dot{\varepsilon}_e}{2\sigma_e}\tau_{rz} \qquad (3d)$$

where the equivalent stress, σ_e, is given by

$$\sigma_e=\frac{1}{\sqrt{2}}\left[(\sigma_r-\sigma_\theta)^2+(\sigma_\theta-\sigma_z)^2+(\sigma_z-\sigma_r)^2+6\tau_{rz}^2\right]^{\frac{1}{2}} \qquad (4)$$

and $\sigma_r,\sigma_\theta,\sigma_z$ and τ_{rz} are the stress components in the directions indicated by subscripts. Furthermore, $\dot{\varepsilon}_e$ is the equivalent strain rate and is defined by Eq. (5), in terms of the strain rate components,

$$\dot{\varepsilon}_e=\frac{\sqrt{2}}{3}\left[(\dot{\varepsilon}_r-\dot{\varepsilon}_\theta)^2+(\dot{\varepsilon}_\theta-\dot{\varepsilon}_z)^2+(\dot{\varepsilon}_z-\dot{\varepsilon}_r)^2+6\dot{\varepsilon}_{rz}^2\right]^{\frac{1}{2}} \qquad (5)$$

where $\dot{\varepsilon}_r,\dot{\varepsilon}_\theta,\dot{\varepsilon}_z$ and $\dot{\varepsilon}_{rz}$ are the strain rate components in the directions indicated by subscripts.

It must be noted that from these three sets of equations, only the equilibrium equations, Eqs. (2a,b), are applicable to both the effective fiber and the matrix. Also, based on the available literature, to satisfy strictly the equilibrium equations, the stress-displacement rate relations, and the essential boundary conditions, solutions for the stress transfer problem require extensive numerical analysis. However, simple analytical solutions are attainable when some of the above equations are satisfied approximately, and the rest of equations are satisfied exactly.

2.3 Boundary conditions

In order to obtain the correct strain rate and stresses of the composite, it is necessary to apply appropriate boundary conditions to the mathematical model. Here, the iso-displacement condition is appropriate for the present problem, see Fig. 2.

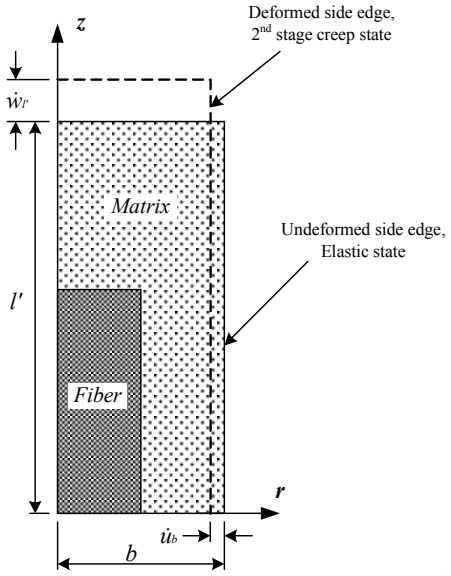

Fig. 2. Schematic of the unit cell edges in the 2nd stage creep and the elastic states

According to the physics of the problem, three sets of boundary conditions, that is the conditions on the border surfaces of the unit cell, the conditions on the fiber/matrix interface

region, and the axial force equilibrium conditions, can be proposed.

The applied boundary conditions on the border surfaces of the unit cell (i.e. $r=0$, $r=b$, $z=0$ and $z=l'$) are given by

$$\dot{u}(b,z)=\dot{u}_b \qquad 0\le z\le l' \qquad (6a)$$

$$\dot{w}(r,0)=0 \qquad a\le r\le b \qquad (6b)$$

$$\tau_{rz}(0,z)=\tau_{rz}(b,z)=0 \qquad 0\le z\le l' \qquad (6c)$$

$$\tau_{rz}(r,0)=\tau_{rz}(r,l')=0 \qquad 0\le r\le b \qquad (6d)$$

As mentioned above $\dot{u}_b$ in Eq. (6a) is the prescribed radial displacement rate on the outer surface ($r=b$), see Fig. 2. Also, the boundary conditions on the fiber-matrix interface (i.e. at $r=a$, $0\le z\le l$) are as

$$\dot{u}(a,z)=0 \qquad (7a)$$

$$\dot{w}(a,z)=0 \qquad (7b)$$

$$\tau_{rz}^{m}(a,z)=\tau_{rz}^{f}(a,z)=\tau_i \qquad (7c)$$

$$\sigma_{r}^{m}(a,z)=\sigma_{r}^{f}(a,z)=\sigma_p \qquad (7d)$$

In fact, due to the elastic behavior of the fiber during the creep deformation of the composite, no matrix slipping on the fiber at the interface is an acceptable assumption. Therefore, both displacement rate components in the radial and axial directions at the interface are zero. Also, according to the shear-lag theory the interfacial shear stress of the fiber and the matrix are equal. Moreover, for a bonded interface, the continuity condition (i.e. Eq. (7d)) is required at the interface.

The axial force equilibrium conditions between the fiber and the matrix at any z location along the model length is presented by

$$\pi b^2\sigma_0=\int_0^a\sigma_z^f(r,z)\mathrm{d}(\pi r^2)+\int_a^b\sigma_z^m(r,z)\mathrm{d}(\pi r^2) \qquad (8a)$$

or in an average manner,

$$b^2\sigma_0=a^2\bar{\sigma}_z^f+(b^2-a^2)\bar{\sigma}_z^m \qquad (8b)$$

where the superscripts m and f denote the respective matrix and fiber and the bar sign on the stress symbol (e.g. $\bar{\sigma}_z^m$) denotes the average value over the cross-sections of the matrix or the fiber.

Since the matrix only creeps, no index of form is given to $\dot{u}$, $\dot{w}$ and $\dot{\varepsilon}_e$ for avoiding complications.

2.4 Solution procedure

For solving such a complex problem, the composite is divided to two separate regions, see Fig. 3.

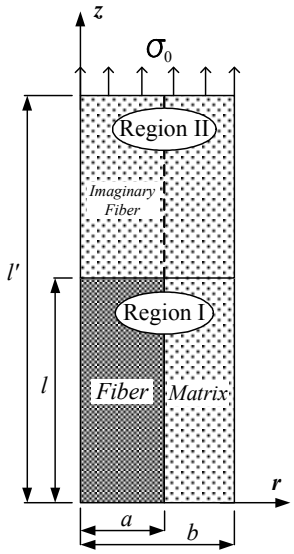

Fig. 3. Illustration of the two important regions for problem solution

Without considering region II, the creep behavior of region I is determined, first. Then by the use of appropriate boundary conditions, the creep strain rate for the full composite model (i.e. regions I plus II) is calculated. The details of the solution procedure are discussed in the following subsections.

2.4.1 Obtaining τ_{rz}^f and τ_{rz}^m in region I

The equation dictating the stress transfer in the shear-lag model and the approximate shear stress distributions in both the fiber and the matrix can be derived from Eq. (2a). Integration of Eq. (2a) over the cross section of the fiber and then division by its cross sectional area πa^2 yield [10-12]:

$$\frac{\mathrm{d}\bar{\sigma}_z^f}{\mathrm{d}z}=-\frac{2}{a}\tau_i \qquad (9)$$

where $\bar{\sigma}_z^f$ is the average value of σ_z^f over the cross-section of the fiber.

To drive the shear stress distribution in the fiber and the matrix, the axial stress gradient is

assumed to be a function of z, and the obtained results are [10-12]

$$\tau_{rz}^{f} = \frac{r}{a}\tau_i \tag{10a}$$

$$\tau_{rz}^{m} = \frac{a}{b^2 - a^2}\left(\frac{b^2}{r} - r\right)\tau_i \tag{10b}$$

The above equations satisfy continuity of the shear stress at the interface, i.e. Eq. (7c), as well as the free surface condition, i.e. Eq. (6d).

2.4.2 *Obtaining $\dot{u}, \dot{w}$ and τ_i in region I*

In this step $\dot{u}$ and $\dot{w}$ and also $\tau_i(z)$, which has remained to be defined from the last step are determined. The incompressibility condition, i.e. adding up the Eqs. (3a-c), will produce

$$\frac{\partial \dot{u}}{\partial r} + \frac{\dot{u}}{r} + \frac{\partial \dot{w}}{\partial z} = 0 \tag{11}$$

The above equation is integrated with respect to r from a to b, i.e. for the effective matrix region, to give

$$\begin{aligned} &\frac{1}{\pi(b^2 - a^2)}\int_a^b \frac{\partial \dot{w}}{\partial z}(2\pi r)\mathrm{d}r \\ &+ \frac{1}{\pi(b^2 - a^2)}\int_a^b \frac{1}{r}\frac{\partial (r\dot{u})}{\partial r}(2\pi r)\mathrm{d}r = 0 \end{aligned} \tag{12}$$

Since the average axial displacement rate over the cross-section of the effective matrix can be defined as

$$\bar{\dot{w}} = \frac{1}{\pi(b^2 - a^2)}\int_a^b \dot{w}(r,z)(2\pi r)\mathrm{d}r \tag{13}$$

considering Eq. (13), Eq. (12) becomes,

$$\frac{\mathrm{d}\bar{\dot{w}}}{\mathrm{d}z} = \frac{-2b}{b^2 - a^2}\dot{u}_b \tag{14}$$

Now, to determine $\dot{u}$, it is assumed that

$$\frac{\partial \dot{w}}{\partial z} = f(z) \tag{15}$$

where $f(z)$ is a function yet to be determined.

Substituting Eq. (15) into Eq. (11) and integrating with respect to r from a to r and applying the corresponding boundary conditions will yield

$$\dot{u} = -\frac{1}{2}\left(r - \frac{a^2}{r}\right)f(z) \tag{16}$$

Then $f(z)$ and thus $\dot{u}$ will be determined by substituting Eq. (6a) to Eq. (16) as

$$f(z) = \frac{-2b}{b^2 - a^2}\dot{u}_b \tag{17a}$$

$$\dot{u} = \frac{b\dot{u}_b}{b^2 - a^2}\left(r - \frac{a^2}{r}\right) \tag{17b}$$

As Eq. (17b) shows, $\dot{u}$ is independent of z coordinate in the matrix region. Hence, this requires that $\dot{u}$ satisfies the following condition,

$$\frac{\partial \dot{u}}{\partial z} = 0 \tag{18}$$

Substituting Eq. (10b) into Eq. (3d), with the use of Eq. (18), gives

$$\frac{\partial \dot{w}}{\partial r} = \frac{3\dot{\varepsilon}_e}{\sigma_e}\left(\frac{b^2}{r} - r\right)\frac{a\tau_i}{b^2 - a^2} \tag{19}$$

Now, using the B.C's on the fiber-matrix interface and substituting Eqs. (7a,b,d) into Eqs. (3a-c) gives

$$\sigma_\theta^m(a,z) = \sigma_z^m(a,z) = \sigma_p \tag{20}$$

Substituting the above equation into Eq. (4) and using Eq. (7c) will give the equivalent stress at the interface as

$$\sigma_e(a,z) = \sqrt{3}\tau_i \tag{21}$$

Now, substituting the above equation into Eq. (1) yields

$$\dot{\varepsilon}_e(a,z) = A\exp\left(\frac{\sqrt{3}}{B}\tau_i\right) \tag{22}$$

The basic assumption in the solution method is introduced by substituting $\dot{\varepsilon}_e(a,z)$ and $\sigma_e(a,z)$ into Eq. (13) for calculating $\dot{w}$ in the domain $(a \le r \le b)$ based on τ_i and as a function of radial coordinate 'r'. This approximation is such that Eq. (19) can be completely satisfied at the interface and the outer surface of the unit cell and also will yield acceptable functions of r for $\dot{w}$ in the domain $(a \le r \le b)$.

Now, by substituting Eqs. (21) and (22) into Eq. (19) one will reach at

$$\frac{\partial \dot{w}}{\partial r} = \frac{\sqrt{3}aA}{(b^2 - a^2)}\left(\frac{b^2}{r} - r\right)\exp\left(\frac{\sqrt{3}}{B}\tau_i\right) \tag{23}$$

Integrating Eq. (23) with respect to r from a to r and using Eq. (7b) will yield

$$\dot{w}(r,z)=\frac{\sqrt{3}aA}{(b^2-a^2)}\left[b^2\ln(r/a)-\frac{r^2-a^2}{2}\right]\times \exp\left(\frac{\sqrt{3}}{B}\tau_i\right) \quad (24)$$

Substituting Eq. (24) into Eq. (13), with the use of Eq. (14), will yield

$$\tau_i(z)=\frac{B}{\sqrt{3}}\ln\left(-\frac{\dot{u}_b}{C}z\right) \quad (25)$$

where C is a constant related to the geometry and material property of the matrix region and can be written as

$$C=\frac{\sqrt{3}\,aA}{2b(b^2-a^2)}\left[b^4\ln\frac{b}{a}+a^2b^2-\frac{3b^4+a^4}{4}\right] \quad (26)$$

Now substituting Eq. (25) into Eq. (24) yield

$$\dot{w}(r,z)=-\frac{\sqrt{3}\,a\,A\dot{u}_b}{C(b^2-a^2)}\left[b^2\ln(r/a)-\frac{r^2-a^2}{2}\right]z \quad (27)$$

Consequently, the strain rate components of the matrix material in region I, ($a\le r\le b$ and $0\le z\le l$), could be obtained.

Substituting Eq. (17b) into Eqs. (3a,b) gives the radial and circumferential strain rates, respectively.

$$\dot{\varepsilon}_r=\frac{b\dot{u}_b}{(b^2-a^2)}\left[1+\frac{a^2}{r^2}\right] \quad (28)$$

$$\dot{\varepsilon}_\theta=\frac{b\dot{u}_b}{(b^2-a^2)}\left[1-\frac{a^2}{r^2}\right] \quad (29)$$

Then, using Eq. (27) in Eq. (3c) will lead to

$$\dot{\varepsilon}_z=-\frac{\sqrt{3}\,a\,A\dot{u}_b}{C(b^2-a^2)}\left[b^2\ln(r/a)-\frac{r^2-a^2}{2}\right] \quad (30)$$

Also, substituting Eqs. (18) and (27) into Eq. (3d) gives the shear strain rate as

$$\dot{\varepsilon}_{rz}=-\frac{\sqrt{3}\,a\,A\dot{u}_b}{2C(b^2-a^2)}\left[\frac{b^2}{r}-r\right]z \quad (31)$$

2.4.3 *Obtaining $\bar{\sigma}_z^f$, $\bar{\sigma}_z^m$ and $\dot{u}_b$*

Now, the rule of mixture equation can be used to calculate $\dot{u}_b$, which is still an unknown parameter. To do this, it is necessary to obtain $\bar{\sigma}_z^f$, first. Therefore, substituting Eq. (25) into Eq. (9) and integrating the obtained equation with respect to z from l to z gives

$$\bar{\sigma}_z^f=-\frac{2Bz}{a\sqrt{3}}\ln\left(-\frac{\dot{u}_b z}{C}\right)-\frac{2B(l-z)}{a\sqrt{3}}+\frac{2Bl}{a\sqrt{3}}\ln\left(-\frac{\dot{u}_b l}{C}\right)+\bar{\sigma}_z^f\Big|_{z=l} \quad (32)$$

where $\bar{\sigma}_z^f\big|_{z=l}$ is the stress acting on the fiber end face ($z=l$), i.e. the end stress.

In the present study, for securing the least possible approximation in the fiber end stress, the behavior of the shear stress in region ($0\le r\le a$ and $l\le z\le l'$) is assumed to be linear. It must be noted that the interfacial shear stress at ($z=l'$) is equal to zero and at ($z=l$) it is found by Eq. (25). Therefore, the shear stress will then be determined as

$$\tau_i'(z)=\frac{(l'-z)}{(l'-l)}\tau_l \quad (33)$$

where the prime sign indicates that the equation is written for the domain mentioned above, which is so called the imaginary fiber region, see Fig. 3.

Therefore, using the shear-lag equation, i.e. Eq. (9) for the mentioned region, one will get

$$\frac{\mathrm{d}\bar{\sigma}_z'^f}{\mathrm{d}z}=-\frac{2}{a}\tau_i' \quad (34)$$

where $\bar{\sigma}_z'^f$ is the average axial stress in the imaginary fiber region.

Substituting Eq. (33) into Eq. (34) and then integrating with respect to z from l to l' and applying the appropriate boundary condition (i.e. $\bar{\sigma}_z'^f\big|_{z=l'}=\sigma_0$) will yield

$$\bar{\sigma}_z^f\Big|_{z=l}=\frac{B(l'-l)}{a\sqrt{3}}\ln\left(-\frac{\dot{u}_b l}{C}\right)+\sigma_0 \quad (35)$$

Now, by substituting Eq. (35) into Eq. (32) the average axial stress in fiber can be given by

$$\bar{\sigma}_z^f=-\frac{2Bz}{a\sqrt{3}}\ln\left(-\frac{\dot{u}_b z}{C}\right)-\frac{2B(l-z)}{a\sqrt{3}}+\frac{B(l'+l)}{a\sqrt{3}}\ln\left(-\frac{\dot{u}_b l}{C}\right)+\sigma_0 \quad (36)$$

Finally, the only unknown parameter, i.e. $\dot{u}_b$, is calculated using the rule of mixture equation as

$$f\overline{\overline{\sigma}}_z^f + (1-f)\overline{\overline{\sigma}}_z^m = \sigma_0 \tag{37}$$

where double bar sign on the stress symbol (i.e. $\overline{\overline{\sigma}}_z^f$ and $\overline{\overline{\sigma}}_z^m$) indicates the averaging of the physical quantity along both r and z directions. therefore, $\overline{\overline{\sigma}}_z^f$ can be expressed as

$$\overline{\overline{\sigma}}_z^f = \frac{1}{l}\int_0^l \overline{\sigma}_z^f \mathrm{d}z \tag{38}$$

Substituting Eq. (36) into Eq. (38) and then integrating the result with respect to z from 0 to l will give

$$\overline{\overline{\sigma}}_z^f = \frac{Bl'}{a\sqrt{3}}\ln\left(-\frac{\dot{u}_b l}{C}\right) - \frac{Bl}{2a\sqrt{3}} + \sigma_0 \tag{39}$$

But $\overline{\overline{\sigma}}_z^m$ could not be calculated with the similar way as used for $\overline{\overline{\sigma}}_z^f$. This is because $\overline{\overline{\sigma}}_z^m$ belongs to the total matrix of the composite model (i.e. regions I and II, Fig. 3). To calculate $\overline{\overline{\sigma}}_z^m$, according to Fig. 2, in the steady state creep stage the volume of the composite remains constant. Therefore, the relationship between the unit cell displacement rates in r and z directions at $r=b$, i.e. $\dot{u}_b$, and $z=l'$, i.e. $\dot{w}_{l'}$, could be found from Eq. (40).

$$\dot{w}_{l'} = -\frac{2l'\dot{u}_b}{b} \tag{40}$$

Hence, the composite creep strain rate can be obtained as

$$\dot{\varepsilon}_c = -\frac{2\dot{u}_b}{b} \tag{41}$$

Note that the calculated creep strain rate will produce an average stress in the matrix as $\overline{\overline{\sigma}}_z^m$, which could be found by substituting Eq. (41) into Eq. (1) as

$$\overline{\overline{\sigma}}_z^m = B\ln\left(-\frac{2\dot{u}_b}{Ab}\right) \tag{42}$$

Now, by substituting Eqs. (39) and (42) in Eq. (37), $\dot{u}_b$ can be obtained as

$$\dot{u}_b = -\frac{Ab}{2} \times \exp\left[\frac{flB + 2a\sqrt{3}(1-f)\sigma_0 - fl'B\ln\left(\frac{Abl}{2C}\right)}{fl'B + a\sqrt{3}B(1-f)}\right] \tag{43}$$

2.4.4 *Obtaining radial, circumferential and axial stresses in region I*

For defining the radial, circumferential and axial stresses in the matrix, substituting Eqs. (3a,b) will result in

$$\sigma_r^m = \frac{2\sigma_e}{3\dot{\varepsilon}_e}\left(2\frac{\partial \dot{u}}{\partial r} + \frac{\dot{u}}{r}\right) + \sigma_z^m \tag{44a}$$

$$\sigma_\theta^m = \frac{2\sigma_e}{3\dot{\varepsilon}_e}\left(\frac{\partial \dot{u}}{\partial r} + 2\frac{\dot{u}}{r}\right) + \sigma_z^m \tag{44b}$$

Substituting the above equations into Eq. (2b) and performing some simplifications gives

$$\sigma_z^m(r,z) = \sigma_p + h(r,z) \tag{45}$$

where

$$h(r,z) = \int_a^r \frac{4B\ln(\dot{\varepsilon}_e/A)}{3\dot{\varepsilon}_e}\frac{\partial \dot{\varepsilon}_z}{\partial r}\mathrm{d}r - \int_a^r (2\dot{\varepsilon}_r + \dot{\varepsilon}_\theta)\frac{\partial}{\partial r}\left[\frac{2B\ln(\dot{\varepsilon}_e/A)}{3\dot{\varepsilon}_e}\right]\mathrm{d}r - \frac{aB}{\sqrt{3}(b^2-a^2)}\left[b^2\ln(r/a) - \frac{r^2-a^2}{2}\right]z \tag{46}$$

Now, the only unknown parameter for calculating $\sigma_z^m(r,z)$ is σ_p, which is a function of z direction only. The average axial normal stress in the matrix for region I can be obtained as

$$\overline{\sigma}_z^m(z) = \frac{1}{\pi(b^2-a^2)}\int_a^b \sigma_z^m(r,z)(2\pi r)\mathrm{d}r \tag{47}$$

Therefore, the interfacial radial pressure, i.e. σ_p, could be calculated by substituting Eq. (45) into Eq. (47) as

$$\sigma_p = \overline{\sigma}_z^m - \frac{2}{b^2-a^2}\int_a^b rh(r,z)\mathrm{d}r \tag{48}$$

where $\overline{\sigma}_z^m$ can be determined by substituting Eq. (36) into Eq. (8b).

Then, the axial stress in the matrix as a function of r and z is found by substituting the above equation into Eq. (45). Due to the

complications involved with Eqs. (46) and (48), calculating the obtained analytical integrations are almost impossible. In the present research work, these integrations are done numerically for the chosen test case, which is discussed in the next section.

4 Results and discussions

To examine the validity of the present analytical model, the SiC/Al6061 composite is chosen as a test case. For comparison purpose, the finite element numerical calculations of creep behavior of this composite are also carried out using the finite element commercial code of ANSYS (version 7.0). The model geometry is chosen as shown in Fig. 1 and the surface conditions are applied as presented in Eqs. (6a-d), see Fig. 2. The axisymmetry approach with nonlinear quadratic element of PLANE 183 is used for FEM analysis. This element is a higher order eight-node element and has creep modeling capability, as well.

For the composite used here (SiC/Al6061), the volume fraction of fibers is 15% and the fibers have an aspect ratio of 7.4 and $k = 0.76$, which are in accordance with the suggestions made in [4]. For more information regarding the experimental measurements of the above factors including the micrographs, one can refer to Ref. [4]. Also, the steady state creep constants of the matrix material, A and B, in Eq. (1) are considered as $A = \exp(-24.7)$ and $B = 6.47$, which are also given in [4].

To present the results it is important to verify the most critical point in this solution, first. This is the relationship between the equivalent stress at the interface $(\sigma_e(a,z))$ and the interfacial shear stress (τ_i) along the fiber length during the secondary creep stage as given by Eq. (21). Then the analytical results of σ_e and τ_{rz} at the outer surface of the unit cell (i.e. at $r = b$) are presented. This is backed by the calculated stress components in the matrix at the outer surface of the unit cell. Also, the average axial stresses in the fiber and matrix in region I will be compared with the FEM results. To do this, it is necessary to verify the interfacial shear stress distribution in the matrix in region II. As was explained in the previous section, to solve the problem, a linear distribution for the shear stress along the model length from the fiber end to the unit cell free surface was assumed.

Then a comparison of the mentioned average stresses and the interfacial shear stress in the elastic and the secondary creep states could highlight the power of the proposed solution technique. This comparison enables one to exactly describe the load transfer mechanism between the fiber and the matrix during the second stage creep and the nature of the stress components in the composite constituents become more easily describable.

What remains to be describe here, are the radial and axial displacement rates (i.e. $\dot{u}, \dot{w}$). This is necessary to be done before talking about $\dot{\varepsilon}_c$. Finally, the creep strain rates calculated by FEM and the presented analytical method vs. different applied constant loads are discussed and also the results will be compared with the available experimental creep measurements of the composite.

2.5 Verification of the stress field components

The results of the analytical and FEM calculations of shear stress and equivalent stress along the fiber length at the interface are shown in Fig. 4. Interestingly, an excellent correlation between the results exists.

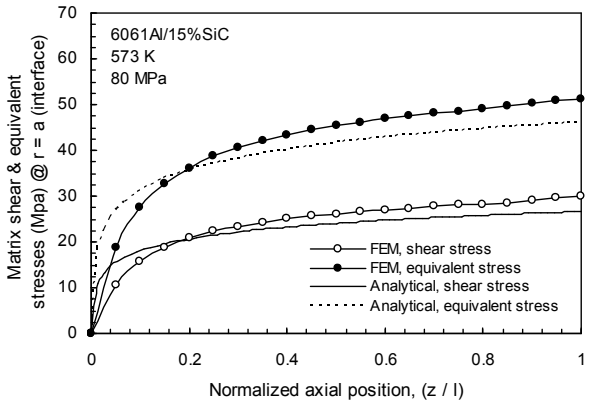

Fig. 4. Analytical and FEM curves of shear and equivalent stresses of matrix in Region I at the interface

The power of the proposed method is further backed by comparison of the analytically calculated σ_e and τ_{rz} at the outer surface of the

unit cell (i.e. at $r = b$) with the FEM results, see Fig. 5. As expected, at the outer surface, $\tau_{rz} = 0$ and σ_e is constant along the fiber, i.e. independent of z.

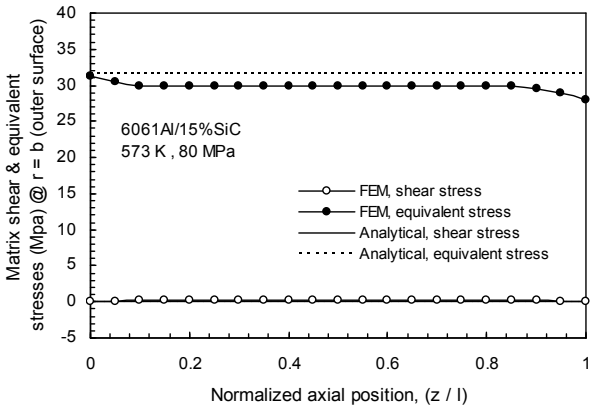

Fig. 5. Analytical and FEM curves of shear and equivalent stresses of matrix in Region I at the outer surface

The analytical and FEM calculations of the axial stress of the matrix along the fiber length at $r = a$ and $r = b$ are shown in Figs. 6. According to the figure, the analytical and FEM results match well.

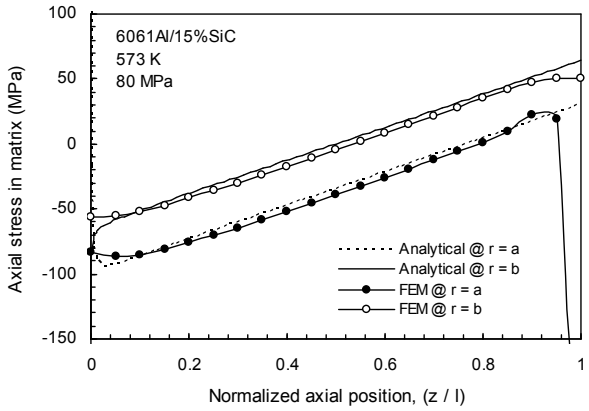

Fig. 6. Analytical and FEM curves of the axial stress in matrix @ $r = a$ and $r = b$

To show the validity of the method for calculating the axial stress in the fiber, the FEM axial stress at five different locations in domain $0 \le r \le a$ along the fiber length and the average analytical axial stress are presented in Fig. 7.

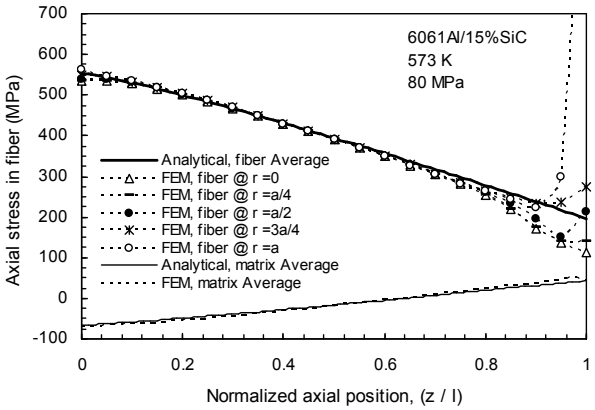

Fig. 7. Analytical and FEM results of the axial stress in fiber and matrix

As it is seen, the calculated average analytical values exactly match the FEM results. Moreover, an excellent match occurs between the analytically calculated average axial stress in the matrix and the FEM results.

Based on Fig. 7, the average axial stress at the fiber end is in a good agreement with the FEM results at ($0 \le r \le a$, $z = l$). This is due to the approximation made for the shear stress in region II at $r = a$. It must be noted that the area under the shear stress curve could be interpreted as the average axial stress at the fiber end (i.e. $\overline{\sigma}_z^f\big|_{z=l}$).

2.6 Verification of the displacement rates

In the current study, according to Eq. (41), the composite creep rate ($\dot{\varepsilon}_c$) could be found using $\dot{u}_b$ without having access to $\dot{w}_{l'}$. Therefore, as a check point for validity of $\dot{\varepsilon}_c$, the distribution of radial and axial displacement rates in region I are verified by the FEM results. Fig. 8 illustrates the radial displacement rate distribution in domain $a \le r \le b$ for both FEM and the analytical method.

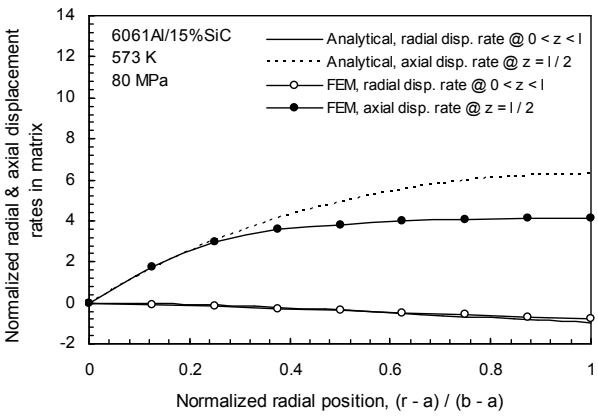

Fig. 8. Analytical and FEM results of radial and axial displacement rates in matrix normalized by $|\dot{u}_b|$ vs. the normalized radial position

Since $\dot{u}$ is independent of z along the fiber length, only the graph for one of the locations is presented here. As it is seen, an excellent correlation exists between the results. Also, Fig. 8 shows both FEM and the analytical calculations of the $\dot{w}$ distribution in $a \le r \le b$ at $z = l/2$. As the figure shows, the shear strain rate values, i.e. $\dot{\gamma}_{rz}$, obtained by both methods coincide well at $r = a$ and $r = b$. This is also backed by the $\dot{w}$ values at $r = b$ along the fiber length as shown in Fig. 9.

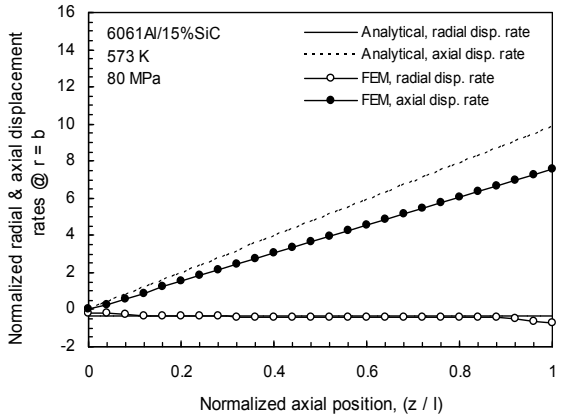

Fig. 9. Analytical and FEM results of axial and radial displacement rates in matrix normalized by $|\dot{u}_b|$ vs. the normalized axial position

However, the small difference in $\dot{w}$ along the radial direction, as the results show, has no effect on the prediction of global behavior of the composite. Also, as it is seen in Fig. 9, the calculated $\dot{u}$ coincides well with the FEM results.

2.7 Verification of the composite creep strain rate

Now, the calculated composite creep strain rate by the present method is compared with the FEM results and the analytical results obtained by Taya-Lilholt [4] under different applied loads σ_0. Table 1 presents the creep strain rate $(\dot{\varepsilon}_c)$ for the three aforementioned studies.

Table 1. Analytical and FEM values of creep strain rate of the composite $(\sigma_0 = 80\ \text{MPa})$

	FEM	Analytical	Taya-Lilholt [4]
$\dot{\varepsilon}_c$	1.04×10^{-9}	0.94×10^{-9}	31.27×10^{-9}

As it is clear, the results in reference [4] are very far from the other two methods. Furthermore, the Taya-Lilholt analytical method is not capable of analyzing the stress and displacement rate fields in the composite as functions of r and z coordinates. The proposed equation by Taya-Lilholt [4] for $\dot{\varepsilon}_c$ of the composite is expressed as

$$\dot{\varepsilon}_c = (1-f)A\exp\left[\frac{\sigma_0/B - C}{1+0.5fs}\right] \qquad (49)$$

where C in the above equation is given by

$$C = 0.5fs\left[\ln s + \ln\eta - 1.193\right] \qquad (50)$$

and η is defined as

$$\eta = \frac{4}{3}\frac{1}{(kf)^{-1/3} - 1} \qquad (51)$$

Now a comparison of the creep results obtained under different applied load σ_0 using the presented analytical method and FEM can show the superiority of the analytical method, further. As Fig. 10 shows, the results obtained match well with the FEM results.

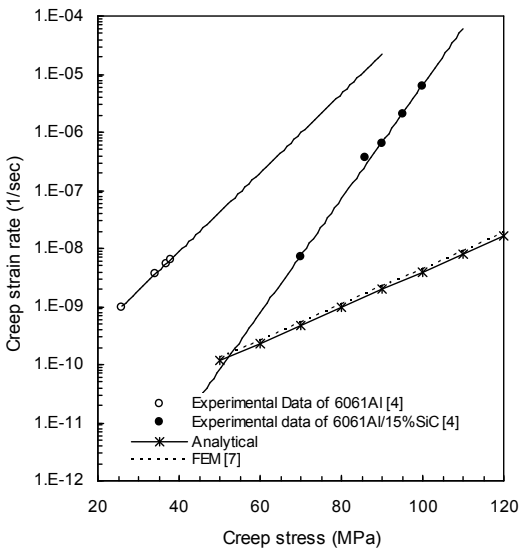

Fig. 10. Comparison of analytical and FEM models prediction with composite creep data for a 6061Al/15%SiC at 573 K, [4]

However, in comparison to the available experimental results of the composite, a big discrepancy is detected between the calculated results and the measurement data specifically at higher applied stresses. As for the reasoning, one is referred to the assumption made by the analytical and numerical methods. Note that the perfect bond at the fiber/matrix interface is not consistent with the microstructure and creep behavior of discontinuous SiC-Al composites at high external applied loads. This has been shown both analytically and numerically [4,7] that with introducing fiber/matrix debonding, the creep prediction by the modeling methods will highly improve. However, since the primary goal here is the development of the analytical approach, this effect is not discussed in the present work.

5 Conclusions

In the present work, a new analytical model for stress analysis and calculation of the steady state creep behavior of short fiber composites subjected to an applied axial load was developed. The analytical model is based on the shear-lag theory with assuming perfect bond at the fiber/matrix interface.

Based on the results obtained so far, it could be concluded that:

1 The matrix stress and displacement rate field components obtained from the proposed analytical solution satisfies the equilibrium and constitutive creep equations. Also, the obtained results satisfy well the overall boundary conditions including the surface conditions, the interface continuity conditions, the axial force equilibrium conditions, and are in a good agreement with the FEM results.

2 The assumption made for the $\dot{\gamma}_{rz}$ distribution in Eq. (23) has no effect on the prediction of the stress and displacement rate components of the short fiber composite.

3 Due to the assumption made for the effective stress and strain rate the proposed method is independent of the chosen creep law.

4 The main advantage of the present method relative to the previous analytical methods like Taya-Lilholt is in its capability of predicting the stress fields and the displacement rate components in the composite and compatibility of the obtained results with the FEM predictions.

References

[1] Kelly A, Street KN. Creep of Discontinuous Fibre Composites. II. Theory for the Steady-State. *Proc R Soc Lon,* pp 283-293, 1972.

[2] Lilholt H. Creep of Fibrous Composite Materials. *Compos Sci Technol*, 22, pp 277-294, 1985.

[3] McLean M. Creep deformation of metal-matrix composites. *Compos Sci Technol*, 23, pp 37-52, 1985.

[4] Morimoto T, Yamaoka T, Lilholt H, Taya M. Second stage creep of silicon carbide whisker/6061 aluminum composite at 573K. *J Eng Mater Technol*, 110, pp 70 76, 1988

[5] Lee YS, Batt TJ, Liaw PK. Stress analysis of a composite material with short elastic fibre in power law creep matrix. *Int J Mech Sci*, 32(10), pp 801-815, 1990.

[6] Wang YR, Chou TW. Analytical modeling of creep of short fiber reinforced ceramic matrix composite. *J Compos Mater,* 26(9), pp 1269-1286, 1992.

[7] Mondali M, Abedian A, Adibnazari S. FEM study of the second stage creep behavior of Al6061/SiC metal matrix composite. *Comput Mater Sci*, 34, pp 140-150, 2005.

[8] Cox HL. The elasticity and strength of paper and other fibrous materials. *Br J Appl Phys*, 3, pp 72 79, 1952.

[9] Boyle JT, Spence J. *Stress analysis for creep*. Southampton: Butterworths Press, p 58, 1983.

[10] Hsueh CH. Interfacial Debonding and Fiber Pull-out Stresses of Fiber-Reinforced Composites. *Mater Sci Eng*, A123(1), pp 1–11, 1990.

[11] Hsueh CH. A Modified Analysis for Stress Transfer in Fiber-Reinforced Composites with Bonded Fiber ends. *J Mater Sci,* 30, pp 219–224, 1995.

[12] Nayfeh AH, Abdelrahman WG. Micromechanical modeling of load transfer in fibrous composites. *Mech Mater,* 30, pp 307–324, 1998.

[13] Jiang Z, Liu X, Li G, Lian J. A new analytical model for three-dimensional elastic stress field distribution in short fibre composite. *Mater Sci Eng*, A366, pp 381–396, 2004.

[14] Abedian A, Mondali M, Pahlavanpour M. Basic modifications in 3D micromechanical modeling of short fiber composites with bonded and debonded fiber end. *Comput Mater Sci*, 40, pp 421–433, 2007.

Copyright Statement